ACS APPLIED BIO MATERIALS

www.acsabm.org Article

3D Flower-like NiCo Layered Double Hydroxides: An Efficient Electrocatalyst for Non-Enzymatic Electrochemical Biosensing of Hydrogen Peroxide in Live Cells and Glucose in Biofluids

Muthaiah Annalakshmi, Sakthivel Kumaravel, Tse-Wei Chen, Shen-Ming Chen,* and Bih-Show Lou*

Cite This: *ACS Appl. Bio Mater.* 2021, 4, 3203−3213 Read Online

ACCESS | Metrics & More | Article Recommendations | Supporting Information

ABSTRACT: Herein, a hierarchical structure of flower-like NiCo layered double hydroxides (NiCo LDH) microspheres composed of three-dimensional (3D) ultrathin nanosheets was successfully synthesized via a facile hydrothermal approach. The formation of NiCo LDH was confirmed by various physicochemical studies, and the NiCo LDH-modified glassy carbon electrode was used as an efficient dual-functional electrocatalyst for non-enzymatic glucose and hydrogen peroxide (H_2O_2) biosensor. The host matrix of hydrotalcite NiCo LDH exhibits the enhanced electrocatalytic sensing performances with a quick response time (<3 s), wide linear range (50 nM−18.95 mM and 20 nM−11.5 mM) and lowest detection limits (S/N = 3) (10.6 and 4.4 nM) toward glucose and H_2O_2, and also it exhibits good stability, selectivity, and reproducibility. In addition, this biosensor was successfully utilized to the real-time detection of endogenous H_2O_2 produced from live cells and glucose in various biological fluids, and demonstrates that the as synthesized NiCo LDH may provide a successful pathway for physiological and clinical pathological diagnosis.

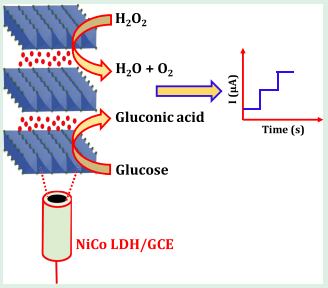

KEYWORDS: *non-enzymatic glucose sensor, hydrogen peroxide sensor, flower-like layered double hydroxides, living cells, 2D nanosheets*

1. INTRODUCTION

One of the increasing research themes in this modern world are the direct electrochemical detection of glucose and hydrogen peroxide (H_2O_2). Generally, diabetes mellitus is one of the top most chronic disease of human beings by increasing blood glucose concentration from the normal level of 80 to 120 mg/dL (4.4−6.6 mM).[1] Hence, it causes several disorders to human bodies including kidney failure, skin, heart, nerve degeneration, and also blindness.[2] In general, more than 422 million adults suffer from diabetes mellitus, which was reported in 2017 by the World Health Organization (WHO) and expected that this result will increase 2-fold from this number by 2030.[3] Therefore, the urgent need to control and the quantitative monitoring of glucose level in human body is highly essential in the clinical diagnosis of diabetes mellitus.

In addition to glucose detection, the rapid and accurate quantification of H_2O_2 has also attracted considerable attention in clinical, biomedical, and environmental analysis. As a reactive oxygen species (ROS), H_2O_2 plays a vital role in several physiological processes including intracellular signaling transduction, cell proliferation, protein synthesis, cell growth, immunity activity, and other living activities, etc.[4] However, the over accumulation of H_2O_2 in cells can cause oxidative stress, cell damages, and produce serious life threatening diseases to human body such as cancer, Alzheimer's, Parkinson's, cardiovascular, and atherosclerosis.[5] For mammals, the calculated physiological level of H_2O_2 is 1 nM, and the maximal intracellular H_2O_2 concentration during peak generation would be 0.5−0.7 μM.[6] Therefore, the precise determination of endogenous H_2O_2 in cellular level is critically important to avoid tumor growth and lethal outbreaks of oxidative stress. Hence, it is emerging as a known biomarker for cancer diagnosis and treatment of diseases, and thus, it would deliver a chance to understanding their physiological and pathological role in biological environments.

In this view, an enormous analytical tool has been developed for the qualitative and quantitative analysis of H_2O_2 and glucose including chromatography,[7] spectrometry,[8] fluorescence,[9] colorimetry,[10] and so on. Nevertheless, most of these developed assays are highly expensive and include tedious and laborious procedure due to their lengthy assay times that always needed an expert operator to handle the complicated analytical procedures and usage of toxic reagents. In contrast, electrochemical transducer-based biosensors have been considered as a promising method due to their high selectivity, rapid responses, ease operation, low detection limit, and real-time monitoring ability in both in vitro and in vivo.[4] Generally, as the characteristics representative of the electrochemical

Received: December 10, 2020
Accepted: March 5, 2021
Published: March 18, 2021

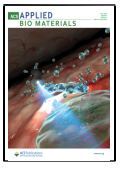

https://dx.doi.org/10.1021/acsabm.0c01600
ACS Appl. Bio Mater. 2021, 4, 3203−3213

Scheme 1. Schematic Representation of the Present Study

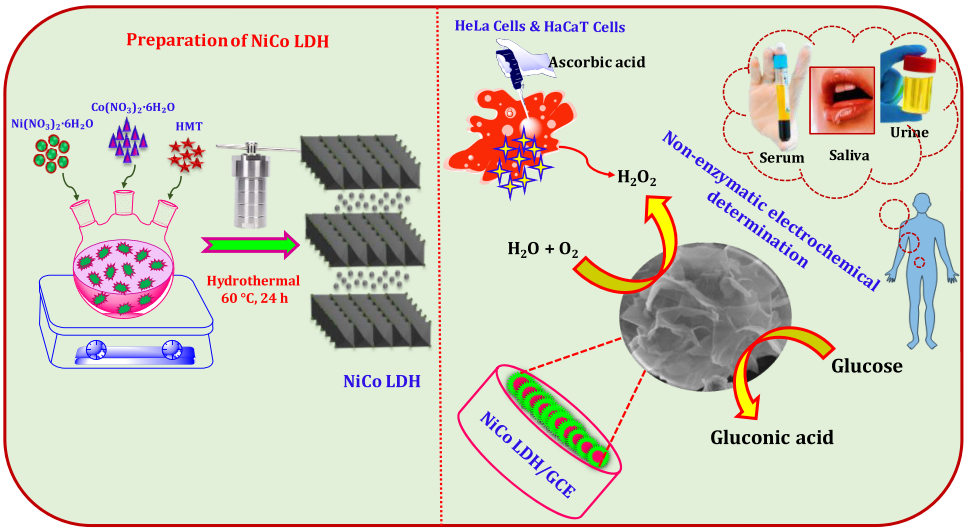

assays, enzyme immobilized electrochemical sensors are found to be very effective owing to their good sensitivity and selectivity. However, owing to their demerits of instability, tedious immobilization procedure, high cost, and low reproducibility, it is still limited.[11] Therefore, the non-enzymatic biosensor-based electrocatalysts have attracted worldwide attention by avoiding these problems toward the electrochemical detection of glucose and H_2O_2.[12] The direct electrochemical sensing performances of H_2O_2 and glucose not only help to transport an electron but also perform a rapid redox process at the electrolyte/electrode surface.[13] For the purpose of developing a highly active electrocatalysts, transition-metal-based materials have created tremendous attention to research scientists toward the non-enzymatic electrochemical biosensors due to their good biocompatibility, high chemical stability, and catalytic activity.[14,15] Recently, first-row transition metal (Fe, Ni, Mn, Cu, and Co)-based oxides,[16] hydroxides,[17] phosphides,[18] dichalcogenides,[19] carbides,[20] and nitrides[21] have been widely used as an alternative electrocatalyst due to their low cost, high stability, earth abundance, and superior electrocatalytic behavior toward the determination of H_2O_2 and glucose. Especially, Ni and Co-based materials have been considered as the most promising electrocatalyst due to their theoretically high catalytic behavior and earth abundance and also the mixed form of Ni and Co systems can provide the synergistic effect on the electrocatalysis.[22]

Specifically, layered double hydroxides (LDH) are a family of two-dimensional lamellar anionic clays made up of both cationic hydrotalcite-like host layers and charge compensating anionic interlayers.[23] In the hydrotalcite layers, both divalent (M^{2+}) and trivalent (M^{3+}) metallic cations are coordinated with the centers of edge-sharing octahedral sites by the hydroxyl groups that are linked to make infinite 2D sheets and then the generic structure of LDH can be written as $[M^{2+}_{1-x}M^{3+}_{x}(OH)_2]_x^{+}[A^{n-}]_{x/n}\ mH_2O$.[24] Due to their unique physiochemical properties of low cost, high electrical conductivity, mechanical stability, flexibility, LDH have been attracting enormous attention in several applications including catalysis,[25] batteries,[26] and supercapacitors.[27] Particularly, the layered structure of LDH possesses high specific surface area owing to the abundant active sites and thus can rapidly promote the electron transfer, hence, this offers a superior electrochemical activity.[28] Redox property of the LDH can be promoted using transition metals (such as Co, Ni, Mn, and Fe), which undergo a Faradaic reaction via an electrochemical pathway in an appropriate potential range.[29] The LDH materials can conduct electricity due to electron hopping between metal centers that are close together or due to displacement of ion outside or inside the material. Therefore, the LDH have been considered as pseudo capacitive materials to produce supercapacitors.[30,31] As compared to the applications of LDH in electrochemical energy storage systems, electrochemical sensing is still limited. Relevant cases such as NiMn-LDH for enzyme-free detection of hydrogen peroxide,[32] NiFe-LDH for the detection of glucose,[33] $Cu(OH)_2$ decorated NiCo-LDH for the electrochemical determination of glucose,[34] and MnO_2 intercalated MgAl LDH for hydrogen peroxide detection[35] have been reported. All these approaches clearly demonstrate that the transition-metal-based LDH (TM-LDH) have superior sensing performances toward the detection of H_2O_2 and glucose can be attributed by the presence of multiple valencies of the two metal ions, which beneficially creates the active sites of donor−acceptor for the electrochemical redox process.[36] Moreover, Shahrokhian *et al.*, proposed $Cu(OH)_2$ decorated NiCo-LDH for the electrochemical sensing of glucose, and compared to this, our prepared NiCo-LDH has more sensitivity.[34] Typically, a variety of synthetic routes have been developed for the preparation of LDH including hydrothermal, microwave assisted, and electrode deposition method etc.[27] Some of these abovesaid methods are unsuitable for the large-scale applications due to the tedious synthetic procedure and resulted compounds have impurities. For this instance, the conventional co-precipitation method in a closed system under hydrothermal conditions is a time-consuming, eco-friendly, and simple method to synthesize the pure 2D and 3D LDH with well-defined morphology and improved catalytic behavior.[37] Moreover, the synthesis of homogeneous precipitation of TM-LDH is somewhat difficult. Conversely, in a hydrothermal condition, as a hydrolysis agent, hexamethylenetetramine (HMT) or urea can be used to prepare the highly crystallized TM-LDH, thus makes the homogeneous crystallization by the change of solution alkaline.[38]

https://dx.doi.org/10.1021/acsabm.0c01600
ACS Appl. Bio Mater. 2021, 4, 3203−3213

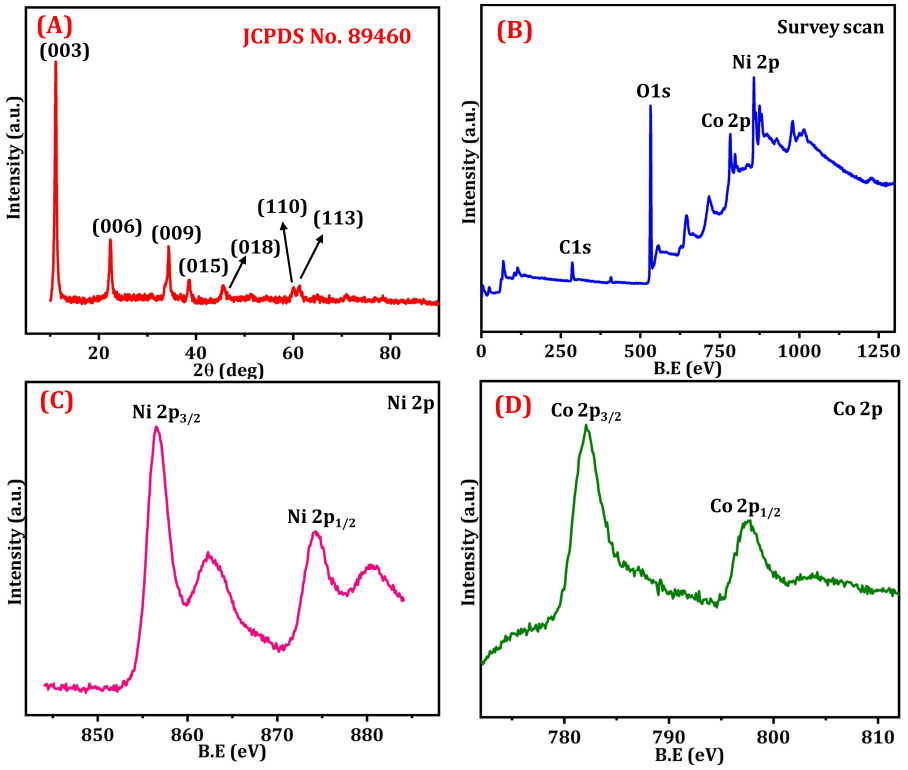

Figure 1. (A) XRD pattern of NiCo LDH, (B) XPS survey spectrum, (C) Ni 2p, and (D) Co 2p for NiCo LDH.

On the basis of the above thought, novel non-enzymatic H_2O_2 and glucose sensors were developed based on the ultrathin two-dimensional (2D) nanosheets interconnected 3D NiCo LDH microflowers. The NiCo LDH was prepared by using hexamethylenetetramine (HMT) as a hydrolysis agent under hydrothermal conditions at low temperature (60 °C) and it was used as an electrode modifier toward the cellular detection of H_2O_2 and glucose sensor. As we expected, the NiCo LDH-modified electrode exhibits an admirable stability and sensitivity toward H_2O_2 and glucose in a broad linear range, along with good selectivity and low detection limits. Hence, it is applied for the practical applications of detection of endogenous H_2O_2 released from live cells and glucose detection in various biological fluids, which is a new horizon for designing better electrocatalysts applied in an electrochemical sensing pathway for pathological and physiological studies. The overall view of a developed biosensor is shown in Scheme 1.

2. EXPERIMENTAL SECTION

2.1. Preparation of NiCo LDH. An efficient and facile hydrothermal approach was used to synthesize a NiCo LDH material. Typically, 0.02 M $Co(NO_3)_2.6H_2O$ and 0.01 M $Ni(NO_3)_2.6H_2O$ were dissolved in 50 mL of deionized water (DIW) at ambient temperature under stirring condition. Then, the HMT solution (0.5 g/20 mL) was added dropwise into this mixture by stirring. Afterward, the homogeneous reaction mixture was poured into a 100 mL stainless-steel Teflon-equipped autoclave for 24 h at 60 °C. After completing the reaction time, autoclave was naturally permitted to cool down to room temperature, then the final products were centrifuged and several times thoroughly washed with DIW/ethanol, and dried overnight at 50 °C in a vacuum oven. Finally, the as-prepared NiCo LDH was used for further physicochemical studies.

2.2. Fabrication Procedure of NiCo LDH-Modified Electrode. To fabricate NiCo LDH, the GCE was thoroughly polished by using alumina powder (0.05 mm) and carefully washed with ethanol and DIW until it achieves a clear surface. Then, 4 mg of NiCo LDH was dispersed in 1 mL of DIW via ultrasonication for 15 min. Next, 6 μL of this suspension was casted on the precleaned GCE surface and then dried using an air oven (50 °C). Finally, the fabricated electrode (NiCo LDH/GCE) was assigned for the detection of non-enzymatic electrochemical glucose and H_2O_2 biosensor.

2.3. Assay Procedure for HaCaT and HeLa Cell Culture. HaCaT cells and the cervical cancer cells, Henrietta Lacks (HeLa), were cultivated with 10% fetal bovine serum (FBS) and L-glutamine in calcium-free Dulbecco's modified Eagle's medium (DMEM). Then, HaCaT cells were further supplemented with calcium chloride and HeLa cells were supplemented with 10% fungizone, penicillin, and streptomycin. Both cells were maintained under a 5% CO_2 humidified atmospheric incubator at 37 °C. After developing to 90% confluency, HaCaT and HeLa cells were separated from DMEM medium by scraping and centrifugation, then a hemocytometer was used to calculate the cell numbers that are calculated as 2×10^6 and 1×10^6. The methodological details of these studies have been followed by the previous studies.[39] Prior to the electrochemical studies, the cells were washed with 0.05 M phosphate buffer (PB) solution (pH 7) three times, and 9 mL of PB solution was used for the quantification of released H_2O_2 by cells at the NiCo LDH-modified electrode.

3. RESULTS AND DISCUSSION

3.1. Characterization of NiCo LDH. To confirm the formed crystalline structure of as-prepared NiCo LDH, the XRD technique was taken and shown in Figure 1A. It shows that the characteristic diffraction peaks at 2θ = 11.12, 22.40, 34. 34, 38.59, 45.68, 60.06, and 61.27° can be well ascribed to the planes of (003), (006), (009), (015), (018), (110), and (113) hydrotalcite-like NiCo LDH phase (JCPDS no. 89-460), respectively. These results are consistent with the previously reported works based on NiCo LDH materials.[40] Moreover, there is no other characteristic peaks were noticed on the XRD patterns, which clearly demonstrates the phase purity and successful formation of NiCo LDH. Also, the obtained results

https://dx.doi.org/10.1021/acsabm.0c01600
ACS Appl. Bio Mater. 2021, 4, 3203−3213

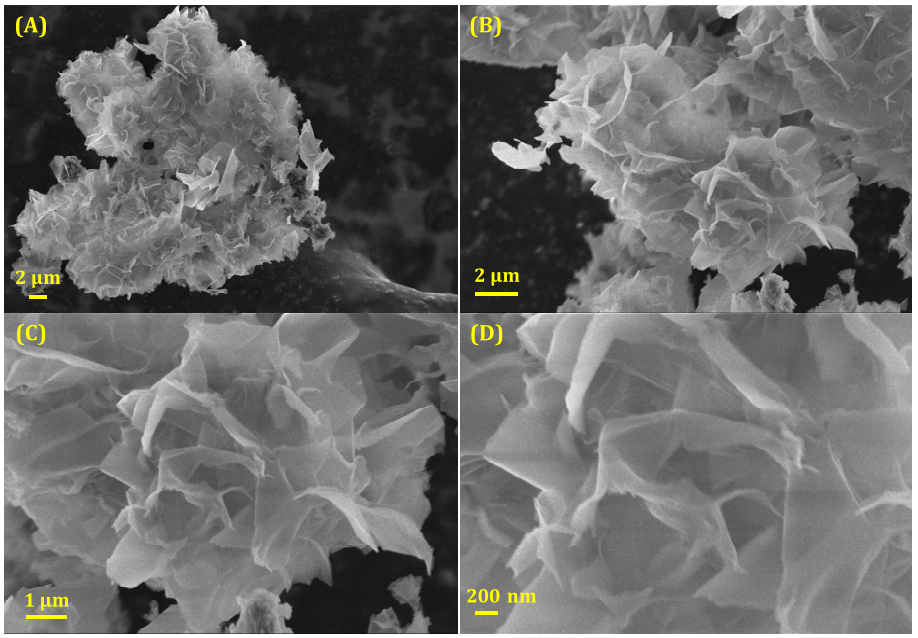

Figure 2. (A–D) FESEM images for NiCo LDH.

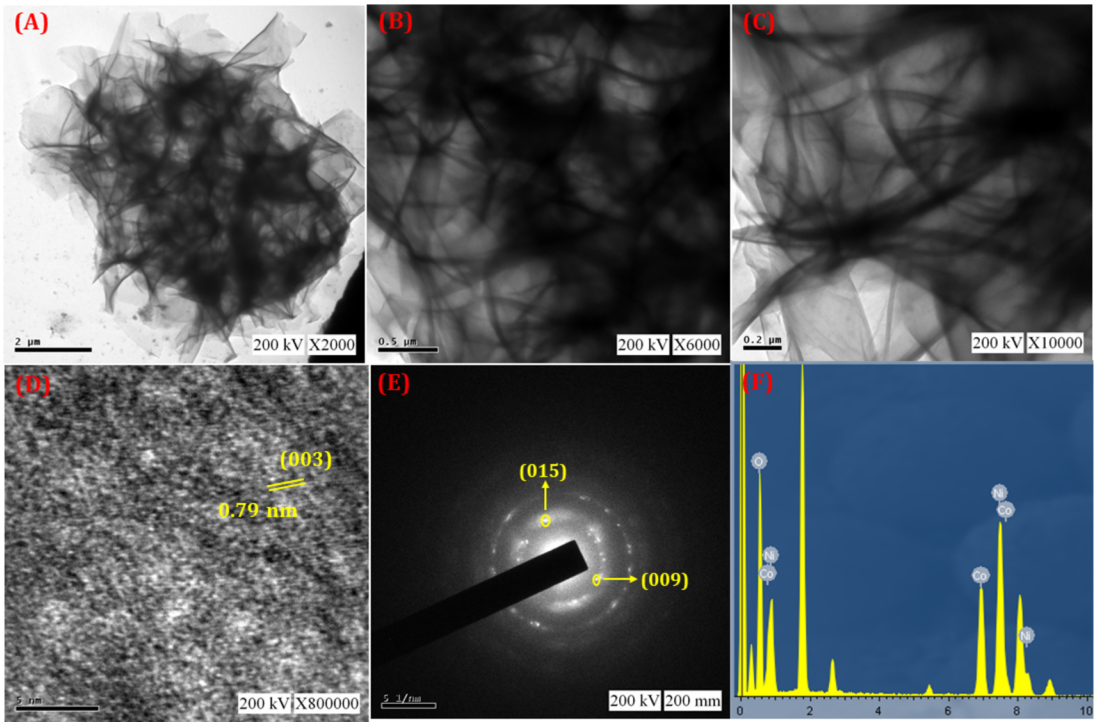

Figure 3. (A–C) TEM images, (D) HRTEM image, (E) SAED pattern, and (F) EDX analysis of NiCo LDH.

are in well accordance with the hydrotalcite-like LDH phase as well as the previously reported literature. According to Braggs law, the calculated *d*-spacing of (d_{003}) is to be 7.9 Å.[41] The average crystalline size can be calculated by using the Scherrer's formula[42]

$$D = K\lambda b \cos\theta$$

where, K is a Scherrer's constant (0.9), D is representing as crystallite size of the NiCo LDH, λ is signified as the wavelength (1.541 Å), and b is a full width half maximum (FWHM) value, which is calculated from the diffraction angle θ. Then, the calculated mean crystalline size of the as-prepared NiCo LDH microflowers is 12.73 nm.

The XPS measurement was scrutinized for the electronic state of elements in the as-prepared NiCo LDH (Figure 1B–D). The high-resolution XPS survey spectrum (Figure 1B) portrays the presence of C, O, Ni, and Co elements on NiCo LDH. The core-level XPS spectra of Ni 2p (Figure 1C) revealed the strong peaks observed for Ni $2p_{1/2}$ and Ni $2p_{3/2}$ at the binding energies of 874.2 and 856.6 eV, respectively, with a spin-energy separation of 17.6 eV and also the two satellite peaks occurred at 862.3 and 880.4 eV, which validates the

https://dx.doi.org/10.1021/acsabm.0c01600
ACS Appl. Bio Mater. 2021, 4, 3203–3213

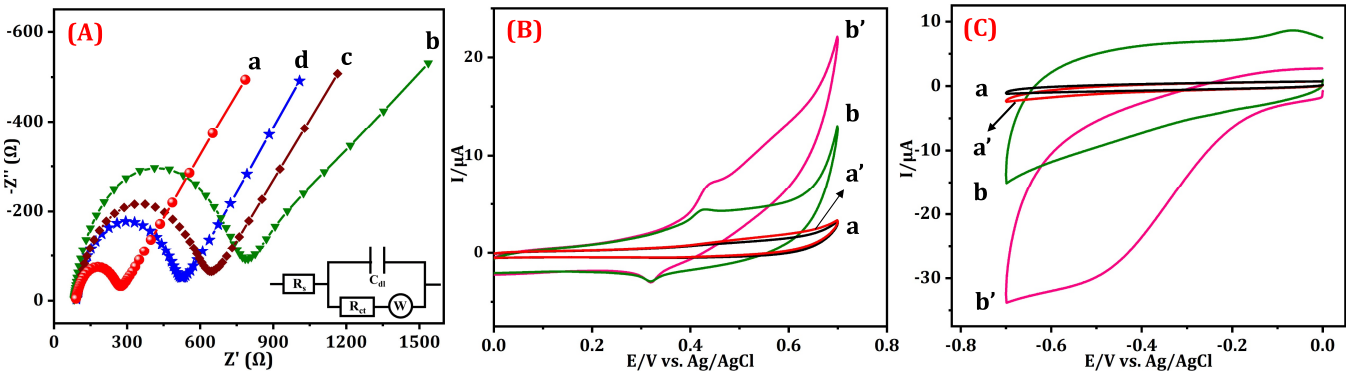

Figure 4. (A) EIS spectrum of various modified and unmodified electrodes in 5 mM $[Fe(CN)_6]^{3-/4-}$ containing 0.1 M KCl, unmodified GCE (a), $Co(OH)_2$/GCE (b), $Ni(OH)_2$/GCE (c), and NiCo LDH/GCE (d). (B) CVs of bare GCE and NiCo LDH-modified electrodes with (a′, b′) and without (a, b) addition of 2 mM glucose at NiCo LDH/GCE in 0.1 M NaOH with a scanning rate of 50 mV s^{-1}, and (C) CVs of bare GCE and NiCo LDH/GCE in the presence (a′, b′) and absence (a, b) of 2 mM H_2O_2 in N_2 saturated 0.05 M PB solution (pH 7) at 50 mV s^{-1}.

existence of Ni^{2+} ions in the LDH structures. Meanwhile, the deconvoluted XPS of Co 2p (Figure 1D) shows the binding energies of 782.1 (Co $2p_{3/2}$) and 797.3 (Co $2p_{1/2}$) with a spin-energy separation of 15.2 eV, respectively, and the intensity of two satellite peaks are pretty low, signifying the coexistence of Co^{2+} and Co^{3+}, which are all in well agreement with early works.[43]

The surface morphology of the as-prepared NiCo LDH is analyzed from FESEM images with different magnifications. As can be seen from the FESEM images of Figure 2A−D, the 3D flower-like hierarchical structure was obtained with smoothie surface. The enlarged FESEM images (Figure 2C,D) reveal that a flower-like microsphere consists of several interconnected petals like 2D nanosheets.[44] The participation of formed 2D networks and the well-defined hybrid flower-like structure moderately boost the mass transfer by creating abundant active sites and also make it as an effective electrocatalyst for the electrochemical redox reactions.

In addition to analyze the morphologies of NiCo LDH, the TEM analysis was performed. Figure 3A−C shows the different magnifications of TEM images, which proves that the microflower-like structures of NiCo LDH are built from many interconnected ultrathin 2D nanosheets, which are developed from the middle and gradually assembled into the complete flower-like structures[44] and also, the TEM images clearly show that the formed ultrathin petal exhibits transparent and flat nature. After that, the high-resolution TEM (HRTEM) (Figure 3D) image revealed the well-arranged lattice fringes that were observed with the interplanar distances of 0.79 nm, which indexed with (003) planes of NiCo LDH. From Figure 3E, it indicates the selective area diffraction (SAED) pattern, which is also validating the formation of NiCo LDH with a *d*-spacing of 0.23 and 0.197 nm and the corresponding planes are (009) and (015), respectively, which is perfectly coordinated with the XRD results. Furthermore, the presence of Ni, Co, and O elements in NiCo LDH were confirmed by the energy dispersive X-ray (EDX) spectrum (Figure 3F) and the corresponding elemental mapping (Figure S1) analysis clearly proving the uniform distribution of Ni, Co, and O throughout the NiCo LDH flower-like structure.

3.2. Electrochemical Properties of the NiCo LDH-Modified Electrode. As the most important powerful analytical technique, electrochemical impedance spectroscopy (EIS) was used to distinguish the interfacial properties between the surface of the modified electrode and bulk solution. Figure 4A shows the typical Nyquist plot of various modified electrodes and the electrolyte solution that consists of 0.1 M KCl containing 5 mM $[Fe(CN)_6]^{3-/4-}$ at under operating frequency range from 0.1 Hz to 100 kHz. The EIS plot was stimulated by using the Randle's circuit model (inset of Figure 4A) and the parameters of R_{ct}, R_s, C_{dl}, and Z_w represent the charge transfer resistance, the electrolyte solute solution of resistance, the interface capacitance, and Warburg impedance, respectively. Moreover, Nyquist plot that is composed of two parts such as semicircle and linear part, which appeared at higher and lower frequencies, could be in accordance with the characteristics of the charge transfer limited and diffusion process at the surface of the electrode.[45] The semicircle diameter (Z′ vs −Z″) of the impedance graph is directly related to the charge transfer resistance (R_{ct}). As shown in Figure.4A, the EIS profile for $Co(OH)_2$/GCE (curve b) and $Ni(OH)_2$/GCE (curve c) shows a much higher semicircle diameter than that of bare GCE (curve a, R_{ct} = 432 Ω), due to the poor electron transfer ability of $Co(OH)_2$ and $Ni(OH)_2$, which hinders the rapid electron transfer of the interface to some extent. As anticipated, the NiCo LDH/GCE (Figure 4A, curve d) showed a much smaller R_{ct} value of 183.3 Ω than the $Co(OH)_2$/GCE (R_{ct} = 705.1 Ω) and $Ni(OH)_2$ (R_{ct} = 546.94), indicating that the rate of charge transfer occurring at the electrode surface is rapid, which can be ascribed to the good ionic conductivity and the lamellar structure of NiCo LDH, which could sufficiently provide a more number of active centers.

To further study the electrocatalytic behavior of NiCo LDH/GCE toward the oxidation of glucose and the reduction of H_2O_2, cyclic voltammetry was conducted in the absence and presence of the target analyte. Figure 4B depicts the CV responses of NiCo LDH/GCE and bare GCE with (a′, b′) and without (a, b) the addition of glucose (2 mM) in 0.1 M NaOH at a scanning range of 50 mV s^{-1}. Obviously, bare GCE (curve a) exhibits no redox peak in the absence (a) of glucose, while there is no significant change was found after the injection of 2 mM glucose (a′) at the bare GCE. On the other hand, a pair of well-defined redox peaks were noted for NiCo LDH/GCE (b) in the absence of glucose at 0.43 and 0.31 V, which is ascribed to the redox reaction of Ni^{2+}/Ni^{3+} in NiCo LDH, under alkaline conditions. Meanwhile, after the addition of 2 mM glucose, the anodic peak current response (I_{pa} = 12 μA; b′) was increased to more than 10-fold than the unmodified GCE at 0.55 V (E_{pa}). For comparison, the $Co(OH)_2$ and $Ni(OH)_2$

https://dx.doi.org/10.1021/acsabm.0c01600
ACS Appl. Bio Mater. 2021, 4, 3203−3213

modified GCE was also assessed for the oxidation of glucose, as depicted in Figure S3A. For $Ni(OH)_2$/GCE (curve a′) and $Co(OH)_2$/GCE (curve b′), considerable current responses were observed toward 2 mM glucose, revealing that $Co(OH)_2$ and $Ni(OH)_2$/GCE has considerable electrocatalytic behavior toward glucose sensing. The plausible glucose oxidation mechanism in the alkaline solution can be written as follows[11,46]

$$Ni^{2+} + OH^- \rightarrow Ni^{3+} + e^- \quad (1)$$

$$Ni^{3+} + \text{glucose} \rightarrow Ni^{2+} + \text{glucolactone} \quad (2)$$

According to the previous reports, the electrocatalytic glucose oxidation at NiCo LDH/GCE surface occurred in the above two steps.[47] In the first step, under alkaline medium, Ni^{3+} is formed due to the electrocatalytic oxidation of Ni^{2+} at the NiCo LDH surface (eq 1). When the glucose is added, the glucose molecules can be electrochemically oxidized into gluconolactone, while in the reverse scan, the Ni^{3+} is reduced to Ni^{2+} (eq 2). Finally, gluconic acid molecules are formed under the alkaline condition via the hydrolysis of gluconolactone molecules, which are desorbed from the electrode.[48] Electrooxidation mechanism of glucose on the NiCo LDH/GCE surface can be seen in Scheme 2.

Scheme 2. Oxidation Mechanism of Glucose at NiCo LDH-Modified GCE Surface

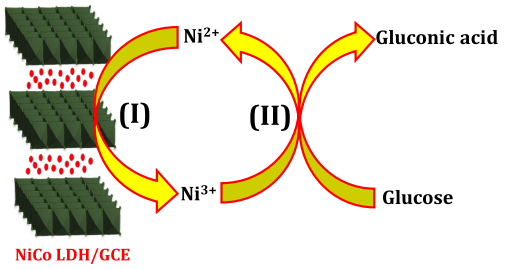

Next, the H_2O_2 sensing properties of bare GCE and NiCo LDH/GCE were employed via CV in N_2 saturated 0.05 M PB solution (pH 7) with the presence (a′, b′) and absence (a, b) of H_2O_2 at 50 mV s^{-1} sweep rate (Figure 4C). From Figure 4C, without the injection of H_2O_2 at bare GCE (a) and NiCo LDH-modified GCE (b) it does not show any noticeable reduction peak current within the potential range from 0 to −0.7 V. However, after the′ addition of 2 mM H_2O_2, the insignificant reduction current response was noted for bare GCE (a′). For comparison, the $Co(OH)_2$ and $Ni(OH)_2$ modified GCE was also assessed toward the sensing of H_2O_2, as depicted in Figure S3B. At $Co(OH)_2$/GCE (4.5 μA; curve a′) and $Ni(OH)_2$/GCE (19 μA; curve b′), substantial current responses were noted with an unsatisfactory current response toward 2 mM H_2O_2, revealing that $Co(OH)_2$ and $Ni(OH)_2$/GCE has considerable electrocatalytic activity for H_2O_2 sensing. As we expected, the remarkable cathodic peak current response was attained at −0.55 V, while the addition of 2 mM H_2O_2 and the reduction peak current (I_{pc} = 30.15 μA; b′) was increased predominantly (28.5-fold) for NiCo LDH/GCE than the bare GCE, $Co(OH)_2$/GCE and $Ni(OH)_2$/GCE. Finally, these results clearly prove that the NiCo LDH had a superior catalytic performance toward glucose oxidation and H_2O_2 reduction. This is due to the high surface-to-volume ratio and synergetic effect of Ni and Co in NiCo LDH. Furthermore, the effect of scan rate on the electrochemical oxidation of glucose and the reduction of H_2O_2 were also studied and given in the Supporting Information (Figure S4).

3.3. Determination of Glucose at the NiCo LDH-Modified Electrode. Furthermore, the NiCo LDH-modified electrode was used to explore the quantitative detection ability of glucose by performing amperometric current-time (i–t) technique. Such quantitative measurement was carried out at a fixed potential of 0.55 V, by adding the sequential injection of various glucose concentrations into continuously stirred (1600 rpm) 0.1 M NaOH at 50 s time interval. The typical i–t response curve shown in Figure 5A, shows a series of stair-step current responses and the considerable increment was noted on the current response after successful injection of 50 nM glucose. The intensity of the response current toward glucose oxidation increased successfully by increasing the consecutive addition of the concentration ranging from 50 nM to 18.95 mM. The maximum steady state current response observed on the NiCo LDH-modified electrode is <3 s, suggesting that the rapid glucose oxidation occurs at the modified electrode surface.[49] A calibration plot between various concentrations of glucose and current response showed a good linearity (Figure 5B). The sensor exhibits the three different linearity such as 50 nM–1.95 mM and 1.95–18.95 mM, respectively, and the correlation coefficient values are R^2 = 0.9916 and R^2 = 0.9949,

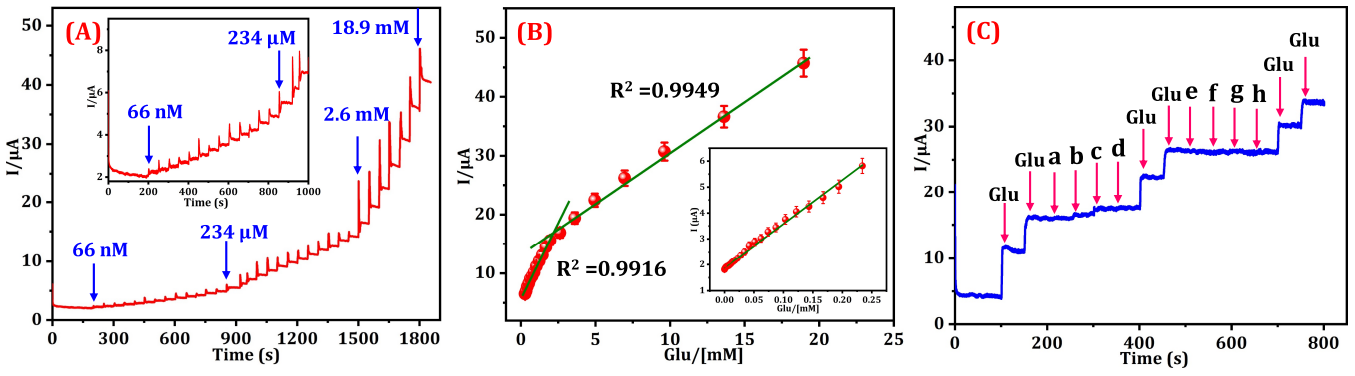

Figure 5. (A) Amperometric current responses to the consecutive addition of glucose in 0.1 M NaOH at a fixed potential of 0.55 V. (B) Linear relationship between the various glucose concentration and oxidation peak currents. (C) I–t responses of the NiCo LDH sensor with the successive injection of H_2O_2 (a), DA (b), UA (c), AA (d), galactose (e), fructose (f), lactose (g), and maltose (h) in the presence of 1 mM glucose containing 0.1 M NaOH at 0.55 V.

https://dx.doi.org/10.1021/acsabm.0c01600
ACS Appl. Bio Mater. 2021, 4, 3203–3213

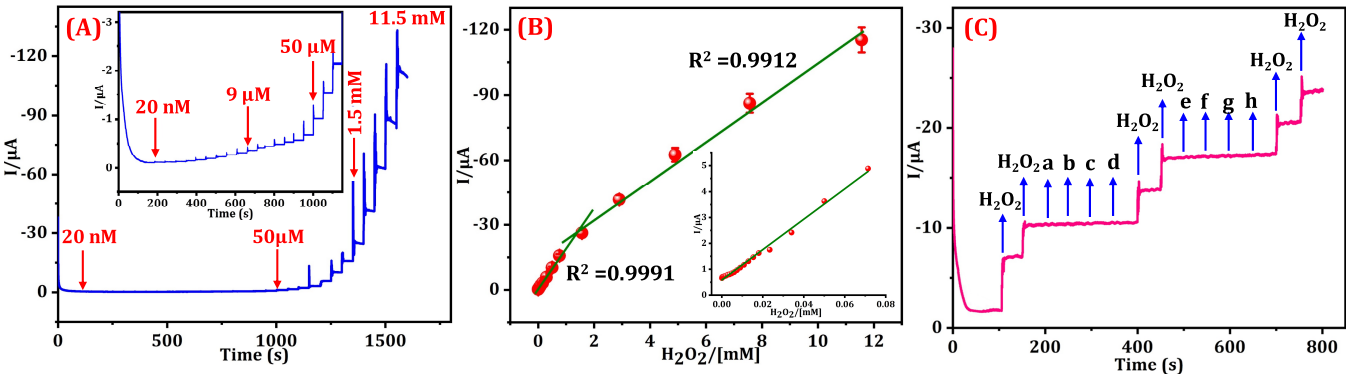

Figure 6. (A) *I*–*t* responses of the NiCo LDH-modified electrode toward the sequential injection of H_2O_2 in N_2 saturated 0.05 M PB solution (pH 7) at a constant potential of −0.5 V. (B) Linear relationship among the reduction peak current vs different concentrations of H_2O_2. (C) Amperometric current responses of the NiCo LDH based biosensor for the successive addition of glu (a), DA (b), AA (c), UA (d), L-cys (e), NaCl (f), KCl (g), and $NaNO_2$ (h) in the presence of 100 μM of H_2O_2 containing N_2 saturated 0.05 M PB solution (pH 7) at −0.5 V.

respectively. The inset in Figure 5B depicts that the linear plot of lowest concentrations of glucose. The limit of detection (LOD) and limit of quantification (LOQ) of the biosensor was estimated from the lowest additions by using the formula, LOD = 3S/N and LOQ = 10S/N (where, S = standard deviation of blank curve and N = slope value)[45] and the calculated values are found to be 10.6 and 35.4 nM, respectively. Then, the obtained sensitivity is 165.66 μA mM^{-1} cm^{-2}. From these results, the linear range of our developed sensor is higher than that of the normal level (4.4–6.6 mM) of glucose in human blood,[50] hence, this assay is not only suitable for the detection of normal range of glucose but also valid for the detection of human blood glucose without using any pretreatments. The obtained analytical parameters toward glucose at NiCo LDH-modified electrodes are more superior to those of other non-enzymatic glucose sensors, as tabulated in Table S1. Such excellent sensing ability can be attributed to the unique microflowers structure with the intercalated lamellar structure, a synergistic property of Ni and Co LDHs.

Furthermore, to confirm the sensing performances of NiCo LDH, it was investigated by the view of anti-interference ability toward glucose oxidation. To demonstrate the anti-interference ability of NiCo LDH, the effect of the response current of some possible electroactive compounds toward glucose was tested via the amperometric method. Because in the practical applications of glucose in blood serum, some possible electrochemically active species such as ascorbic acid (AA), dopamine (DA), uric acid (UA), and other carbohydrates may coexist with the anodic current response of glucose.[8] Figure 5C displays the amperometric current response of 1 mM glucose followed by the excessive addition (3-fold) of aforesaid interfering compounds such as H_2O_2 (a), DA (b), UA (c), AA (d), and various carbohydrates like galactose (e), fructose (f), lactose (g), and maltose (h) in 0.1 M NaOH. From these results, there are no noteworthy signals were found upon the addition of coexisting species. However, the response current of glucose was increased apparently for each addition, and this suggests the remarkable selectivity of NiCo LDH/GCE for the determination of glucose in the presence of potentially active species.

3.4. Electrochemical Detection of H_2O_2 at the NiCo LDH-Modified Electrode. Furthermore, we use the NiCo LDH as an auspicious electrocatalyst to examine the sensing ability toward the reduction of H_2O_2, and amperometric experiment was carried out at an applied potential of −0.5 V. As depicted, Figure 6A reveals the typical amperometric current response for sequential addition of H_2O_2 in N_2 saturated pH 7 (0.05 M PB solution) under continuous stirring. The rapid current responses were achieved with the successive injection of various H_2O_2 concentrations (20 nM–11.5 mM) and 95% of the steady state current was observed within <3 s, and it can be ascribed that the rapid diffusion of H_2O_2 is stimulated on the active sites of the NiCo LDH surface.[51] According to Figure 6A, the response current of H_2O_2 reduction was increased consecutively with increasing the successive injection of H_2O_2. The calibration plot among the reduction peak current (I_{pc}) and several H_2O_2 concentrations is revealed in Figure 6B, and it showed two linearity (20 nM–1.5 mM and 1.5–11.5 mM) with the regression coefficient (R^2) values of 0.9991 and 0.9912. The detection limit (LOD) and limit of quantification (LOQ) were calculated as 4.4 and 14.8 nM at the signal-to-noise ratio, and the obtained sensitivity is 352.263 μA mM^{-1} cm^{-2}. The obtained analytical features such as LOD and broad linear range were compared with the previously developed non-enzymatic sensors, tabulated in Table S2. Even though these proposed sensors have showed good performances, but the complicated synthetic procedure and high-cost electrocatalyst, are still limited. To conclude, the developed NiCo LDH-based sensor possesses superior sensing ability than the other developed sensor. Hence, it has been considered as an auspicious electrocatalyst for the analysis of cellular H_2O_2.

To alleviate the quality of the developed H_2O_2 sensor, the anti-interference property should be studied, which is a major challenge for the electrochemical sensing applications. The selectivity of the sensor was evaluated through the amperometric technique by the injection of various possible interfering species such as glucose (glu), ascorbic acid (AA), dopamine (DA), L-cysteine (L-cys), uric acid (UA), NaCl, KCl, and $NaNO_2$ into 100 μM H_2O_2 containing N_2 saturated PB solution (0.05 M) at the NiCo LDH-modified electrode. Figure 6C demonstrates that the rapid well-defined response current was observed while H_2O_2 was added, whereas there is no noticeable current change was noted for the excessive addition (5-fold) of coexisting species of glu (a), DA (b), AA (c), UA (d), L-cys (e), NaCl (f), KCl (g), and $NaNO_2$ (h). These results imply that the as-prepared NiCo LDH-modified electrode had good tolerance property and selectively determine H_2O_2 even in the presence of 5-fold excessive

https://dx.doi.org/10.1021/acsabm.0c01600
ACS Appl. Bio Mater. 2021, 4, 3203–3213

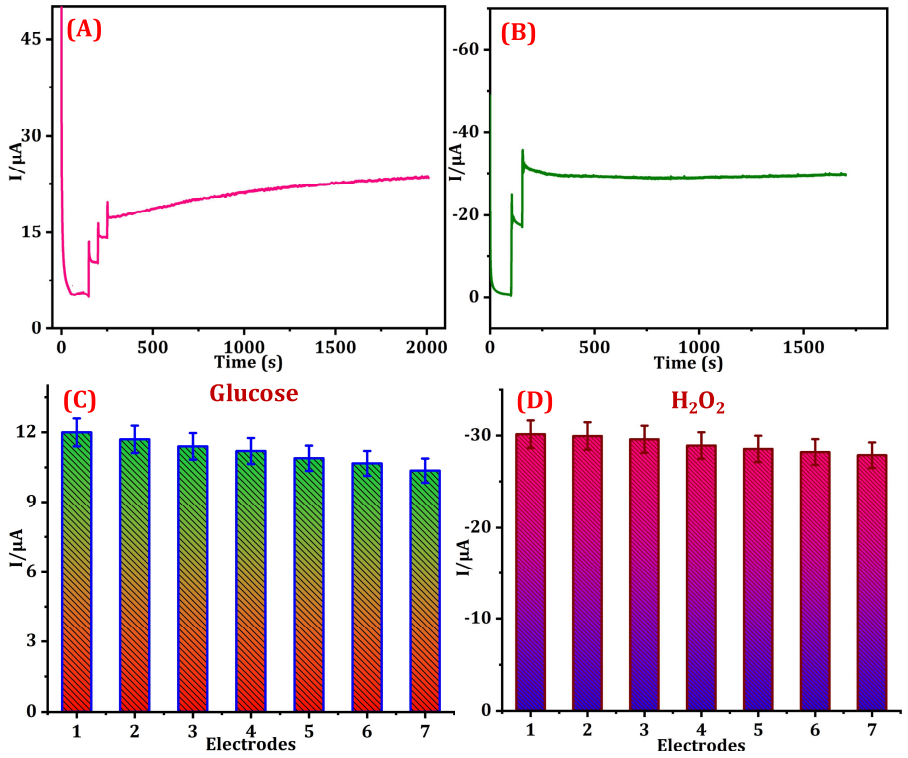

Figure 7. (A) Operational stability of the NiCo LDH-modified electrode toward glucose oxidation. (B) Operational stability of the NiCo LDH-modified electrode toward the reduction of H_2O_2. Reproducibility of NiCo LDH /GCE toward glucose oxidation (C) and H_2O_2 reduction (D).

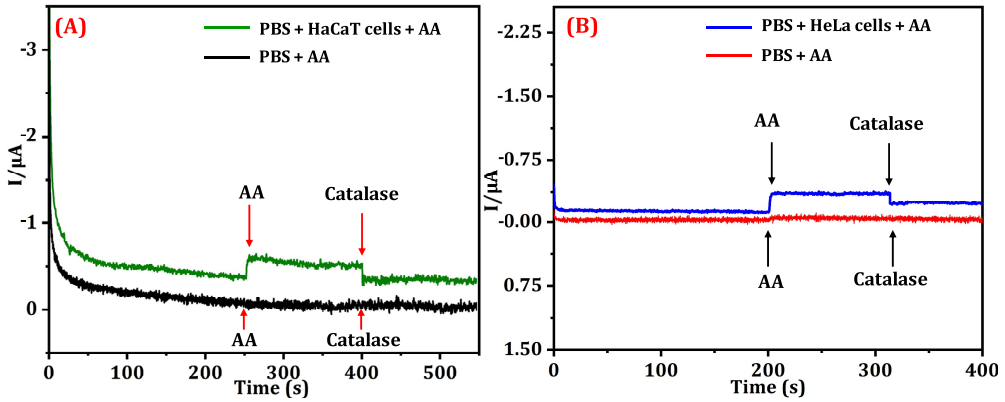

Figure 8. Amperometric *i*−*t* responses for the endogenous H_2O_2 released from living non-cancerous HaCaT cells (A) and cancerous HeLa cells (B) in N_2 saturated PB solution (0.05 M; pH 7) on the NiCo LDH-modified electrode at −0.5 V.

amount of interfering species. Hence, the NiCo LDH/GCE was efficaciously used for the determination of endogenous H_2O_2 secreted from live cells.

3.5. Stability and Reproducibility of the NiCo LDH-Modified GCE. So as to further access the stability of the NiCo LDH-modified electrode, amperometric technique was performed over a long period toward the target analytes. As seen from the amperometric signal (Figure 7A) for 1 mM glucose, the oxidation current retained 96.5% of its initial value over 2000 s. As the same procedure, the stability of NiCo LDH/GCE was also tested by monitoring the reduction current response of 2 mM H_2O_2 over 1700 s. As shown in Figure 7B, after 1700 s, the response current was still maintained at about 97% of its original level. The reproducibility of the NiCo LDH/GCE toward glucose and H_2O_2 was assessed by notifying the current responses at seven different NiCo LDH/GCE samples and the results are revealed in Figure 7C,D. The calculated RSD values are 2.03 and 2.12%, respectively, for glucose and H_2O_2. Finally, all these results clearly proved that our proposed sensor had good operational stability, adequate reproducibility with satisfactory results, hence, it had a great potential to be applied for the practical applications.

3.6. Real-Time Monitoring of Endogenous H_2O_2 in Living Cells. In recent years, cancer is one of the top most disease causes of death worldwide. As an ROS of H_2O_2 is an important molecular product that linked with various in vivo cell functions and it has been recently recognized as an effective biomarker for early cancer diagnosis.[52] Therefore, the NiCo LDH-modified GCE was used as an effective electrode modifier toward real-time quantification of H_2O_2 from both living non-cancer cell (HaCaT) and human cervical cancer cell (HeLa cells). After cultivating by the appropriate reported procedures, the cells were tested via amperometric *i*−*t*

https://dx.doi.org/10.1021/acsabm.0c01600
ACS Appl. Bio Mater. 2021, 4, 3203−3213

technique in N_2 saturated PB solution (0.05 M; pH 7) under an optimal potential of −0.5 V. In general, the level of H_2O_2 increased quickly after the stimulation of cells than the normal levels. Therefore, as per the previous reports, ascorbic acid (AA) that was used as a stimulator can disrupt the redox process of cells to release a greater number of H_2O_2.[53] As shown in the amperometric $i-t$ curve (Figure 8A,B), there is no response current was found when AA was added, and also a scavenger of catalase was added into the electrolyte solution (absence of cell; curve black in Figure 8A and curve red in Figure 8B). In contrast, a significant current response was achieved, when the injection of 10 μM AA into the PB solution containing HaCaT (curve green) and HeLa cells (curve blue) was performed, which suggests that the current increment is only caused by the releasing of H_2O_2 from HaCaT and HeLa cells by stimulating with AA. Subsequently, catalase (300 U/mL) was added into the both cells to confirm the production of H_2O_2, then the current response was dropped almost to a background level, as can be seen from Figure 8A,B due to the decomposition of H_2O_2 fleetly by catalase. The current increment was about 0.231 and 25 μA, corresponding to 0.18 and 2.04 μM H_2O_2, respectively, for non-cancerous HaCaT and cancerous HeLa, which was consistent with previous reports.[39,53] These results declare that the tendency of cancerous cells released large amount of H_2O_2 than the normal cells due to their quick oxygen metabolism, which indicates that the abnormal growth of tumor have an enhancement of ROS, thus, it is a great significance for the applications of cancer diagnosis. Hence, the NiCo LDH-based biosensor possessed good sensing ability toward H_2O_2 detection in living cells and could be hypothetically useful for pathological and physiological studies.

3.7. Determination of Glucose in Biological Fluids. To investigate the practical feasibility of the NiCo LDH-modified electrode for the determination of glucose in several biological fluids (human saliva, urine, and blood serum samples), the samples were tested. The samples were collected from a healthy volunteer, and the results were compared with the commercial glucometer. Prior to analysis, the samples were diluted with 0.1 M NaOH, and the glucose concentration was examined via using the standard addition method through the addition of known concentration of glucose. Then, the amperometric experiments were carried out for different concentrations and the results are summarized in Table 1. The acceptable recoveries were obtained in the range of 98.7−100.06% (blood serum), 99.9−100.3% (urine), and 98.9−100.2% (saliva). The obtained results are in well accordance with a commercial glucometer. Hence, the NiCo LDH-modified electrode can be utilized as a superior electrocatalyst for the practical applicability of glucose.

Table 1. Real-Time Detection of Glucose in Various Biological Fluid

sample	added (mM)	found (mM)	recovery (%)	compared (mM)	RSD (%)
blood serum	1	0.987	98.7	1.002	1.05
	3	2.985	99.5	3.017	0.71
	5	5.003	100.06	5.034	1.32
urine	1	0.999	99.9	1.001	0.71
	3	3.01	100.3	3.005	1.32
	5	4.998	99.96	5.005	0.52
saliva	1	0.989	98.9	1.001	0.46
	3	3.002	100.06	3.002	0.12
	5	5.01	100.2	5.007	0.84

4. CONCLUSIONS

In summary, ultrathin hierarchical flower-like structure of NiCo LDH has been proven as an effective bifunctional electrode material toward the detection of H_2O_2 and glucose. The flower-like structure is made up of participation of numerous interconnected 2D nanosheets. As compared to other developed non-enzymatic glucose and H_2O_2 sensors, our proposed sensor possessed good linearity (50 nM−18.95 mM and 20 nM−11.5 mM), low detection limit (10.6 and 4.4 nM), good selectivity, excellent stability, and adequate reproducibility toward glucose and H_2O_2. The superior electrochemical sensing behavior can be attributed to the mixed transition metal ions that results in a greater number of active sites than the single metal hydroxides, and thus facilitates the fast electron transfer ability and boosts their electrical conductivity. To demonstrate the practical applications of the NiCo LDH based sensor, it was utilized to the quantitative determination of H_2O_2 produced from live cells (HaCaT and HeLa) and the determination of glucose in various biofluids. Hence, these results will promote the exploration of transition-metal-based layered materials that can be effectively used in electrochemical sensors.

■ ASSOCIATED CONTENT

Supporting Information

The Supporting Information is available free of charge at https://pubs.acs.org/doi/10.1021/acsabm.0c01600.

Materials and methods, electrochemical experiments for the developed biosensor, effect of catalyst loading, effect of pH toward H_2O_2, repeatability, cytotoxicity assay, and comparison table for glucose and H_2O_2 sensor (PDF)

■ AUTHOR INFORMATION

Corresponding Authors

Shen-Ming Chen − *Department of Chemical Engineering and Biotechnology, National Taipei University of Technology, Taipei 106, Taiwan, ROC;* orcid.org/0000-0002-0132-9161; Email: smchen78@ms15.hinet.net

Bih-Show Lou − *Department of Nuclear Medicine and Molecular Imaging Center, Chang Gung Memorial Hospital, Taoyuan 33305, Taiwan, ROC; Chemistry Division, Center for General Education, Chang Gung University, Taoyuan 33302, Taiwan, ROC*; Email: blou@mail.cgu.edu.tw

Authors

Muthaiah Annalakshmi − *Department of Chemical Engineering and Biotechnology, National Taipei University of Technology, Taipei 106, Taiwan, ROC*

Sakthivel Kumaravel − *Department of Chemical Engineering and Biotechnology and Institute of Biochemical and Biomedical Engineering, National Taipei University of Technology, Taipei 106, Taiwan, ROC*

Tse-Wei Chen − *Department of Materials, Imperial College London, London SW7 2AZ, UK*

Complete contact information is available at: https://pubs.acs.org/10.1021/acsabm.0c01600

Notes

The authors declare no competing financial interest.

https://dx.doi.org/10.1021/acsabm.0c01600
ACS Appl. Bio Mater. 2021, 4, 3203−3213

■ ACKNOWLEDGMENTS

The authors are thankful for the financial assistance (MOST 107-2113-M-027-005-MY3 and MOST109-2221-E-182-031) from the Ministry of Science and Technology, Taiwan and the Chang Gung Memorial Hospital through the contract no. CMRPD5K0011.

■ REFERENCES

(1) Ngo, Y.-L. T.; Sui, L.; Ahn, W.; Chung, J. S.; Hur, S. H. $NiMn_2O_4$ spinel binary nanostructure decorated on three-dimensional reduced graphene oxide hydrogel for bifunctional materials in non-enzymatic glucose sensor. *Nanoscale* **2017**, *9*, 19318−19327.

(2) Zhu, Z.; Garcia-Gancedo, L.; Flewitt, A. J.; Xie, H.; Moussy, F.; Milne, W. I. A critical review of glucose biosensors based on carbon nanomaterials: carbon nanotubes and graphene. *Sensors* **2012**, *12*, 5996−6022.

(3) Zhang, P.; Zhang, X.; Brown, J.; Vistisen, D.; Sicree, R.; Shaw, J.; Nichols, G. Global healthcare expenditure on diabetes for 2010 and 2030. *Diabetes Res. Clin. Pract.* **2010**, *87*, 293−301.

(4) Zhang, R.; Chen, W. Recent advances in graphene-based nanomaterials for fabricating electrochemical hydrogen peroxide sensors. *Biosens. Bioelectron* **2017**, *89*, 249−268.

(5) Dai, H.; Lü, W.; Zuo, X.; Zhu, Q.; Pan, C.; Niu, X.; Liu, J.; Chen, H.; Chen, X. A novel biosensor based on boronic acid functionalized metal−organic frameworks for the determination of hydrogen peroxide released from living cells. *Biosens. Bioelectron* **2017**, *95*, 131−137.

(6) Zhu, L.; Zhang, Y.; Xu, P.; Wen, W.; Li, X.; Xu, J. PtW/MoS_2 hybrid nanocomposite for electrochemical sensing of H_2O_2 released from living cells. *Biosens. Bioelectron* **2016**, *80*, 601−606.

(7) Gimeno, P.; Bousquet, C.; Lassu, N.; Maggio, A.-F.; Civade, C.; Brenier, C.; Lempereur, L. High-performance liquid chromatography method for the determination of hydrogen peroxide present or released in teeth bleaching kits and hair cosmetic products. *J. Pharm. Biomed. Anal.* **2015**, *107*, 386−393.

(8) Ali, A.; Hussain, Z.; Arain, M. B.; Shah, N.; Khan, K. M.; Gulab, H.; Zada, A. Development of microwave assisted spectrophotometric method for the determination of glucose. *Spectrochim. Acta A* **2016**, *153*, 374−378.

(9) Wen, F.; Dong, Y.; Feng, L.; Wang, S.; Zhang, S.; Zhang, X. Horseradish peroxidase functionalized fluorescent gold nanoclusters for hydrogen peroxide sensing. *Anal. Chem* **2011**, *83*, 1193−1196.

(10) Chen, S.; Hai, X.; Chen, X.-W.; Wang, J.-H. In situ growth of silver nanoparticles on graphene quantum dots for ultrasensitive colorimetric detection of H_2O_2 and glucose. *Anal. Chem* **2014**, *86*, 6689−6694.

(11) Wang, X.; Zheng, Y.; Yuan, J.; Shen, J.; Hu, J.; Wang, A.-J.; Wu, L.; Niu, L. Three-dimensional NiCo layered double hydroxide nanosheets array on carbon cloth, facile preparation and its application in highly sensitive enzymeless glucose detection. *Electrochim. Acta* **2017**, *224*, 628−635.

(12) Bianchi, R. C.; da Silva, E. R.; Dall 'Antonia, L. H.; Ferreira, F. F.; Alves, W. A. A nonenzymatic biosensor based on gold electrodes modified with peptide self-assemblies for detecting ammonia and urea oxidation. *Langmuir* **2014**, *30*, 11,464−11,11473.

(13) Minteer, S. D.; Atanassov, P.; Luckarift, H. R.; Johnson, G. R. New materials for biological fuel cells. *Mater. Today* **2012**, *15*, 166−173.

(14) Zhu, H.; Li, L.; Zhou, W.; Shao, Z.; Chen, X. Advances in non-enzymatic glucose sensors based on metal oxides. *J. Mater. Chem. B* **2016**, *4*, 7333−7349.

(15) Zheng, Y.; Qiao, J.; Yuan, J.; Shen, J.; Wang, A.-J.; Gong, P.; Weng, X.; Niu, L. Three-dimensional NiCu layered double hydroxide nanosheets array on carbon cloth for enhanced oxygen evolution. *Electrochim. Acta* **2018**, *282*, 735−742.

(16) Muench, F.; Sun, L.; Kottakkat, T.; Antoni, M.; Schaefer, S.; Kunz, U.; Molina-Luna, L.; Duerrschnabel, M.; Kleebe, H.-J.; Ayata, S.; Roth, C.; Ensinger, W. Free-Standing Networks of Core−Shell Metal and Metal Oxide Nanotubes for Glucose Sensing. *ACS Appl. Mater. Interfaces* **2016**, *9*, 771−781.

(17) Asif, M.; Haitao, W.; Shuang, D.; Aziz, A.; Zhang, G.; Xiao, F.; Liu, H. Metal oxide intercalated layered double hydroxide nanosphere: with enhanced electrocatalyic activity towards H_2O_2 for biological applications. *Sens. Actuators B Chem.* **2017**, *239*, 243−252.

(18) Tong, S.; Li, Z.; Qiu, B.; Zhao, Y.; Zhang, Z. Biphasic nickel phosphide nanosheets: Self-supported electrocatalyst for sensitive and selective electrochemical H_2O_2 detection and its practical applications in blood and living cells. *Sens. Actuators B Chem.* **2018**, *258*, 789−795.

(19) Cooray, M. C. D.; Zhang, X.; Zhang, Y.; Langford, S. J.; Bond, A. M.; Zhang, J. Cobalt selenide nanoflake decorated reduced graphene oxide nanocomposite for efficient glucose electro-oxidation in alkaline medium. *J. Mater. Chem. A* **2017**, *5*, 19289−19296.

(20) Annalakshmi, M.; Balasubramanian, P.; Chen, S.-M.; Chen, T.-W. Enzyme-free electrocatalytic sensing of hydrogen peroxide using a glassy carbon electrode modified with cobalt nanoparticle-decorated tungsten carbide. *Microchim. Acta* **2019**, *186*, 265.

(21) Xie, F.; Cao, X.; Qu, F.; Asiri, A. M.; Sun, X. Cobalt nitride nanowire array as an efficient electrochemical sensor for glucose and H_2O_2 detection. *Sens. Actuators B Chem.* **2018**, *255*, 1254−1261.

(22) Asadian, E.; Shahrokhian, S.; Zad, A. I. Highly sensitive nonenzymetic glucose sensing platform based on MOF-derived NiCo LDH nanosheets/graphene nanoribbons composite. *J. Electroanal. Chem* **2018**, *808*, 114−123.

(23) Wang, Q.; O'Hare, D. Recent advances in the synthesis and application of layered double hydroxide (LDH) nanosheets. *Chem. Rev* **2012**, *112*, 4124−4155.

(24) He, S.; An, Z.; Wei, M.; Evans, D. G.; Duan, X. Layered double hydroxide-based catalysts: nanostructure design and catalytic performance. *Chem. Commun* **2013**, *49*, 5912−5920.

(25) Sels, B.; De Vos, D.; Buntinx, M.; Pierard, F.; Kirsch-De Mesmaeker, A.; Jacobs, P. Layered double hydroxides exchanged with tungstate as biomimetic catalysts for mild oxidative bromination. *Nature* **1999**, *400*, 855.

(26) Wang, Q.; Shang, L.; Shi, R.; Zhang, X.; Zhao, Y.; Waterhouse, G. I. N.; Wu, L.-Z.; Tung, C.-H.; Zhang, T. NiFe Layered Double Hydroxide Nanoparticles on Co, N-Codoped Carbon Nanoframes as Efficient Bifunctional Catalysts for Rechargeable Zinc−Air Batteries. *Adv. Energy Mater.* **2017**, *7*, 1,700,467.

(27) Patel, R.; Park, J. T.; Patel, M.; Dash, J. K.; Gowd, E. B.; Karpoormath, R.; Mishra, A.; Kwak, J.; Kim, J. H. Transition-metal-based layered double hydroxides tailored for energy conversion and storage. *J. Mater. Chem. A* **2018**, *6*, 12−29.

(28) Li, M.; Cheng, J. P.; Wang, J.; Liu, F.; Zhang, X. B. The growth of nickel-manganese and cobalt-manganese layered double hydroxides on reduced graphene oxide for supercapacitor. *Electrochim. Acta* **2016**, *206*, 108−115.

(29) Gualandi, I.; Vlamidis, Y.; Mazzei, L.; Musella, E.; Giorgetti, M.; Christian, M.; Morandi, V.; Scavetta, E.; Tonelli, D. Ni/Al layered double hydroxide and carbon nanomaterial composites for glucose sensing. *ACS Appl. Nano.- Mater.* **2019**, *2*, 143−155.

(30) Liu, X.-M.; Zhang, Y.-H.; Zhang, X.-G.; Fu, S.-Y. Studies on Me/Al-layered double hydroxides (Me = Ni and Co) as electrode materials for electrochemical capacitors. *Electrochim. Acta* **2004**, *49*, 3137−3141.

(31) Moolayadukkam, S.; Thomas, S.; Sahoo, R. C.; Lee, C. H.; Lee, S. U.; Matte, H. S. S. R. Role of Transition Metals in Layered Double Hydroxides for Differentiating the Oxygen Evolution and Non-enzymatic Glucose Sensing. *ACS Appl. Mater. Interfaces* **2020**, *12*, 6193−6204.

(32) Zhou, J.; Min, M.; Liu, Y.; Tang, J.; Tang, W. Layered assembly of NiMn-layered double hydroxide on graphene oxide for enhanced non-enzymatic sugars and hydrogen peroxide detection. *Sens. Actuators, B* **2018**, *260*, 408−417.

(33) Lu, Y.; Jiang, B.; Fang, L.; Fan, S.; Wu, F.; Hu, B.; Meng, F. Highly sensitive nonenzymatic glucose sensor based on 3D ultrathin NiFe layered double hydroxide nanosheets. *Electroanalysis* **2017**, *29*, 1755−1761.

https://dx.doi.org/10.1021/acsabm.0c01600
ACS Appl. Bio Mater. 2021, 4, 3203−3213

(34) Shahrokhian, S.; Sanati, E. K.; Hosseini, H. Advanced on-site glucose sensing platform based on a new architecture of free-standing Hollow $Cu(OH)_2$ Nanotubes decorated with CoNi-LDH Nanosheets on Graphite Screen-Printed Electrode. *Nanoscale* **2019**, 12655.
(35) Asif, M.; Aziz, A.; Dao, A. Q.; Hakeem, A.; Wang, H.; Dong, S.; Zhang, G.; Xiao, F.; Liu, H. Real-time tracking of hydrogen peroxide secreted by live cells using MnO_2 nanoparticles intercalated layered doubled hydroxide nanohybrids. *Anal. Chim. Acta* **2015**, *898*, 34−41.
(36) Yuan, C.; Wu, H. B.; Xie, Y.; Lou, X. W. D. Mixed transition-metal oxides: design, synthesis, and energy-related applications. *Angew. Chem. Int. Ed.* **2014**, *53*, 1488−1504.
(37) Song, F.; Hu, X. Exfoliation of layered double hydroxides for enhanced oxygen evolution catalysis. *Nat. Commun* **2014**, *5*, 4477.
(38) Han, Y.; Liu, Z.-H.; Yang, Z.; Wang, Z.; Tang, X.; Wang, T.; Fan, L.; Ooi, K. Preparation of Ni^{2+} − Fe^{3+} layered double hydroxide material with high crystallinity and well-defined hexagonal shapes. *Chem. Mater* **2008**, *20*, 360−363.
(39) Annalakshmi, M.; Kumaravel, S.; Chen, S.-M.; Chen, T.-W. Thermo-regulated synthesis of NiMn layered double hydroxides for real-time determination of hydrogen peroxide in living cells and oxidase activity. *Appl. Surf. Sci.* **2021**, *539*, 148256.
(40) Wang, G.; Li, Y.; Zhao, T.; Jin, Z. Phosphatized mild-prepared-NiCo LDHs cabbage-like spheres exhibit excellent performance as a supercapacitor electrode. *New Journal of Chemistry* **2021**, *45*, 251−261.
(41) Waterhouse, G. I. N.; Waterland, M. R. Opal and inverse opal photonic crystals: fabrication and characterization. *Polyhedron* **2007**, *26*, 356−368.
(42) Sangili, A.; Annalakshmi, M.; Chen, S.-M.; Balasubramanian, P.; Sundrarajan, M. Synthesis of silver nanoparticles decorated on core-shell structured tannic acid-coated iron oxide nanospheres for excellent electrochemical detection and efficient catalytic reduction of hazardous 4-nitrophenol. *Compos. B. Eng* **2019**, *162*, 33−42.
(43) Chen, H.; Hu, L.; Chen, M.; Yan, Y.; Wu, L. Nickel−cobalt layered double hydroxide nanosheets for high-performance supercapacitor electrode materials. *Adv. Funct. Mater* **2014**, *24*, 934−942.
(44) Chen, J.; Sheng, Q.; Wang, Y.; Zheng, J. Dispersed Nickel Nanoparticles on Flower-like Layered Nickel-Cobalt Double Hydroxides for Non-enzymic Amperometric Sensing of Glucose. *Electroanalysis* **2016**, *28*, 979−984.
(45) Annalakshmi, M.; Kumaravel, S.; Chen, S.-M.; Balasubramanian, P.; Balamurugan, T. S. T. A straightforward ultrasonic-assisted synthesis of zinc sulfide for supersensitive detection of carcinogenic nitrite ions in water samples. *Sens. Actuators, B Chem* **2020**, *305*, 127387.
(46) Wang, L.; Miao, X.; Qu, Y.; Duan, C.; Wang, B.; Yu, Q.; Gao, J.; Song, D.; Li, Y.; Yin, Z. Rattle-type Au@ NiCo LDH hollow core-shell nanostructures for nonenzymatic glucose sensing. *J. Electroanal. Chem* **2020**, *858*, 113810.
(47) Ni, G.; Cheng, J.; Dai, X.; Guo, Z.; Ling, X.; Yu, T.; Sun, Z. Integrating Ultrathin Polypyrrole Framework on Nickel-Cobalt Layered Double Hydroxide as an Amperometric Sensor for Non-enzymatic Glucose Determination. *Electroanalysis* **2018**, *30*, 2366−2373.
(48) Toi, P. T.; Trung, T. Q.; Dang, T. M. L.; Bae, C. W.; Lee, N.-E. Highly electrocatalytic, durable, and stretchable nanohybrid fiber for on-body sweat glucose detection. *ACS Appl. Mater. Interfaces* **2019**, *11*, 10707−10717.
(49) Dhara, K.; Mahapatra, D. R. Electrochemical nonenzymatic sensing of glucose using advanced nanomaterials. *Microchim. Acta* **2018**, *185*, 49.
(50) Su, Y.; Luo, B.; Zhang, J. Z. Controllable cobalt oxide/Au hierarchically nanostructured electrode for nonenzymatic glucose sensing. *Anal. Chem* **2016**, *88*, 1617−1624.
(51) Dhara, K.; Mahapatra, D. R. Recent advances in electrochemical nonenzymatic hydrogen peroxide sensors based on nanomaterials: a review. *J. Mater. Sci* **2019**, 12319−12357.
(52) Miller, E. W.; Tulyathan, O.; Isacoff, E. Y.; Chang, C. J. Molecular imaging of hydrogen peroxide produced for cell signaling. *Nat. Chem. Biol* **2007**, *3*, 263.
(53) Fu, Y.; Huang, D.; Li, C.; Zou, L.; Ye, B. Graphene blended with SnO_2 and Pd-Pt nanocages for sensitive non-enzymatic electrochemical detection of H_2O_2 released from living cells. *Anal. Chim. Acta* **2018**, *1014*, 10−18.

https://dx.doi.org/10.1021/acsabm.0c01600
ACS Appl. Bio Mater. 2021, 4, 3203−3213